Research Repository UCD

Title	Doping characterization of InAs/GaAs quantum dot heterostructure by cross-sectional scanning capacitance microscopy
Authors(s)	Zhao, Z. Y, Zhang, W. M., Yi, C, Rodriguez, Brian J., et al.
Publication date	2008-03-03
Publication information	Zhao, Z. Y, W. M. Zhang, C Yi, Brian J. Rodriguez, and et al. “Doping Characterization of InAs/GaAs Quantum Dot Heterostructure by Cross-Sectional Scanning Capacitance Microscopy.” American Institute of Physics, March 3, 2008. https://doi.org/10.1063/1.2889938.
Publisher	American Institute of Physics
Item record/more information	http://hdl.handle.net/10197/5204
Publisher's statement	The following article appeared in Applied Physics Letters, 92 (9) : 092101 and may be found at http://link.aip.org/link/doi/10.1063/1.2889938. The article may be downloaded for personal use only. Any other use requires prior permission of the author and the American Institute of Physics.
Publisher's version (DOI)	10.1063/1.2889938

Downloaded 2026-05-01 23:36:53

The UCD community has made this article openly available. Please share how this access benefits you. Your story matters! (@ucd_oa)

© Some rights reserved. For more information

APPLIED PHYSICS LETTERS **92**, 092101 (2008)

Doping characterization of InAs/GaAs quantum dot heterostructure by cross-sectional scanning capacitance microscopy

Z. Y. Zhao,[1] W. M. Zhang,[1] C. Yi,[1] A. D. Stiff-Roberts,[1,a)] B. J. Rodriguez,[2] and A. P. Baddorf[2]

[1]*Department of Electrical and Computer Engineering, Duke University, Durham, North Carolina 27708, USA*

[2]*Center for Nanophase Materials Sciences, Oak Ridge National Laboratory, Oak Ridge, Tennessee 37831, USA*

(Received 11 December 2007; accepted 1 February 2008; published online 3 March 2008)

In order to better understand dopant incorporation in quantum dot infrared photodetectors, the application of cross-sectional scanning capacitance microscopy (SCM) has been used to investigate carrier occupation/distribution in a multilayer InAs/GaAs quantum dot (QD) heterostructure for different doping techniques. The doping schemes in the QD structure include direct doping (in InAs QD layers) and remote doping (in GaAs barrier layers), each with different doping concentrations. The SCM image suggests that large band bending occurs due to highly doped, remote-doping layers, thereby causing electron redistribution in direct-doping layers. The experimental result is supported by a band structure calculation using the Schrödinger–Poisson method by NEXTNANO3. © *2008 American Institute of Physics*. [DOI: 10.1063/1.2889938]

In order to decrease dark current density and to improve spectral response tunability of InAs/GaAs quantum dot infrared photodetectors (QDIPs) at higher operation temperature, it is critical to understand how dopants are incorporated into and transport in quantum dot (QD) active regions. In our previous studies, polarization-dependent Fourier transform infrared (FTIR) spectroscopy, temperature-dependent dark current measurements,[1–3] and capacitance-voltage spectroscopy[4] have been used to study Si dopant incorporation in InAs/GaAs QDIPs. However, the information obtained from these studies is based on macroscopic electrical and optical characterization techniques. Microscopic, spatial information on dopant incorporation in QDs is still lacking. Scanning capacitance microscopy (SCM) has been used as a promising tool for high-resolution, two-dimensional dopant distribution mapping in a variety semiconductor structures, especially Si-based[5,6] devices due to the low defect density of the silicon oxide layer. Recently, the SCM technique has been used for doping studies in III-V compound semiconductor[7,8] devices, as well. This application has been more challenging due to the relatively high defect density in III-V semiconductor oxide layers. However, a thin native oxide layer formed in ambient condition has been reported for a SCM scan on a GaAs/AlGaAs laser mesa buried in GaInP by regrowth.[9] While some works have been conducted to study planar QDs using SCM in both vacuum[10] and ambient[11] conditions, the SCM technique has not been used in a cross-sectional study of doping in QD structures. The current work is unique in the sense that (i) cross-sectional SCM mapping of dopant distribution in a multilayer QD sample provides a spatial representation of dopant incorporation relevant to QDIP operation and (ii) the heterostructure of the multilayer InAs/GaAs QD sample is designed to enable a comparison between direct doping in InAs QD layers and remote doping in GaAs barrier layers featuring different doping concentrations. This application of cross-sectional SCM to evaluate doping in a QD heterostructure demonstrates a technique to enable better understanding of the doping effect on carrier occupation and transport in QDIPs.

A multilayer InAs/GaAs QD heterostructure was designed and grown on a semi-insulating (100) GaAs substrate by solid source molecular beam epitaxy (MBE) using a Riber 2300 system and standard growth techniques.[12] First, an undoped 50 nm $Al_{0.5}Ga_{0.5}As$ marker layer was grown between two undoped 120 nm GaAs buffer layers to provide a reference for selective etching. Next, six single InAs QD layers with different doping schemes and doping concentrations were grown. Each single QD layer was separated by a 120 nm GaAs barrier layer. The bottom three dot layers were directly doped in the InAs QDs, while the top three dot layers were remotely doped over 4 nm thickness in the GaAs barrier 2 nm above the InAs QD layer. With the exception of the remotely doped GaAs spacer layers, all other GaAs layers in the heterostructure were undoped, with unintentional *p*-type doping levels on the order of $10^{14}/\text{cm}^3$.[13] The doping concentrations for both the direct- and remote-doping QDs were selected such that the nominal QD carrier occupations in the three dot layers were 12, 6, and 2 electrons/dot, respectively, from bottom to top. Therefore, the corresponding doping concentrations were calculated by considering the QD surface density, measured to be $\sim 10^{11}$ dots/cm^2 by atomic force microscopy (AFM). For the direct-doping layers, the doping concentrations in the 2.2 ML (or ~6.6 Å) InAs QDs were $2.04\times10^{19}/\text{cm}^3$ (12 electrons/dot), $1.02\times10^{19}/\text{cm}^3$ (6 electrons/dot), and $3.4\times10^{18}/\text{cm}^3$ (2 electrons/dot). For the remote-doping layers, the doping concentrations in the 4 nm GaAs spacer layers were $3\times10^{18}/\text{cm}^3$ (12 electrons/dot), $1.5\times10^{18}/\text{cm}^3$ (6 electrons/dot), and $5\times10^{17}/\text{cm}^3$ (2 electrons/dot). Finally, a thick (1 μm) GaAs cap layer was grown on top of the structure to protect the QD layers from damage during the cleaving process. A schematic diagram of the heterostructure for the bottom six QD layers is shown in Fig. 1.

a)Author to whom correspondence should be addressed. Electronic mail: astiff@ee.duke.edu.

This article is copyrighted as indicated in the abstract. Reuse of AIP content is subject to the terms at: http://scitation.aip.org/termsconditions. Downloaded to IP: 137.43.140.249 On: Fri, 22 Nov 2013 16:01:03

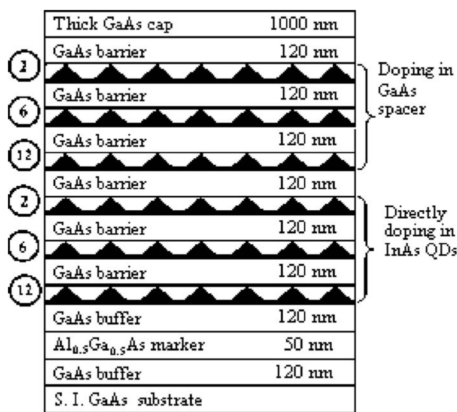

FIG. 1. Schematic diagram of InAs/GaAs QD heterostructure grown by MBE for cross-sectional SCM measurement. The numbers in the circles on the left of the figure show the doping concentration (measured by number of electrons provided for each dot) of each individual layer.

After MBE growth, the sample was cleaved and etched for 15 s using 1:40 (volume) hydroxylamine (30 wt %) and hydrogen peroxide (35 wt %).[14] The etching rate for InAs QD layers (less than 1 nm/s) is lower than the etching rate for GaAs barrier layers (about 2 nm/s). Therefore, the InAs QD layers are higher than the GaAs barrier layers on the etched heterostructure cross section. An Ohmic contact was formed between the etched cross-section sample and a gold plated Si substrate using a melted indium dot at 300 °C. A Veeco NanoScope V scanning probe microscope was used to conduct both cross-sectional AFM and SCM imaging in this experiment. The cross-sectional AFM was used for a reference comparison to the SCM-generated image. Figure 2(a) shows a tapping mode AFM image (2×2 μm^2) of the etched cross-sectional surface of the QD heterostructure, and Fig. 2(b) shows the cross-sectional height profile along the dashed line shown in the AFM image. The contrast in the cross-sectional AFM image results from the different etching rates between InAs and GaAs, with the bright areas corresponding to InAs and the dark areas corresponding to GaAs. The InAs QD layers and the 120 nm GaAs barrier layers are

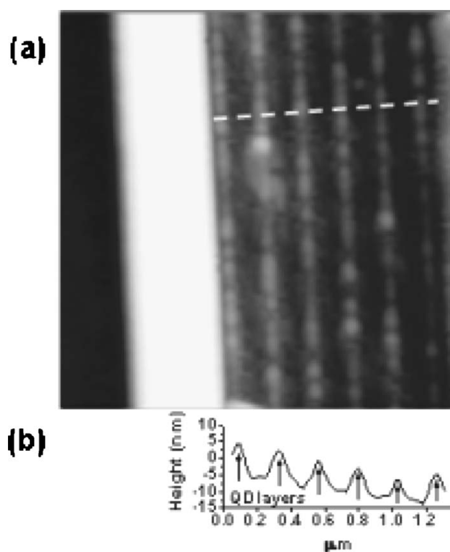

FIG. 2. (a) Cross-sectional AFM image (2×2 μm^2) of etched QD heterostructure for comparison to measured SCM profile and (b) corresponding cross-sectional height profile of the InAs and GaAs layers along the dashed line shown in (a).

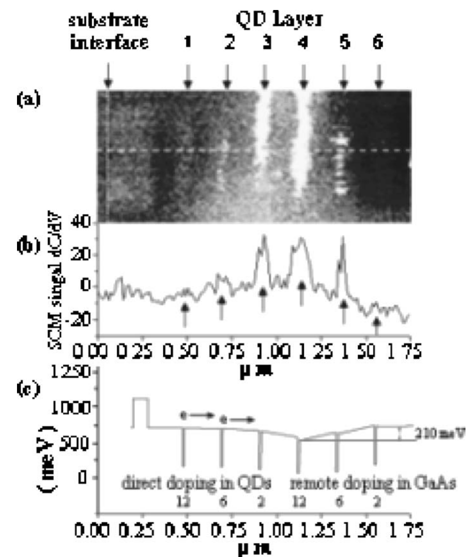

FIG. 3. (a) Cross-sectional SCM image (0.8×1.75 μm^2) of etched QD heterostructure. (b) SCM signal profile along the dashed line in (a). (c) Calculated bandstructure obtained from 3D effective-mass Schrödinger–Poisson method using the NEXTNANO3 semiconductor nanostructure simulation package developed by Walter Schottky Institute. The numbers under the band structure show the doping concentration (measured by number of electrons provided for each dot) of each individual layer.

observed clearly from the AFM image. However, it is important to note that the bottom GaAs buffer layer appears to have a different etching rate compared to the subsequent GaAs barrier layers. This difference in contrast could be due to the presence of the $Al_{0.5}Ga_{0.5}As$ marker layer, which could have some impact on the etching rate of the GaAs buffer layers.

The cross-sectional SCM measurements were carried out on the same sample surface area, using native oxide on the sample surface as a thin insulator layer.[9] Fig. 3(a) shows the cross-sectional SCM image (0.8×1.75 μm^2), which was obtained by raster scanning the tip from the left to right, in the growth direction, beginning at the bottom of the image shown. Doped-diamond-coated *n*-type Si cantilevers with 25 nm radius of curvature and a spring constant of 3 N/m under contact mode scanning were used in the SCM measurement. The measurements were performed under dark conditions in the dC/dV mode with a 2 V dc bias voltage and a 0.15 V ac modulation voltage with 45 kHz modulation frequency. It is important to note that the magnitude of the SCM signal measured in dC/dV mode should be inversely proportional to the free carrier concentration in the region, i.e., bright regions correspond to low-doped areas and dark regions correspond to high-doped areas.[6] However, depending on the sample surface and scanning conditions, a phenomenon known as contrast reversal can occur. This SCM artifact will be discussed in more detail later with respect to Fig. 3.

The QD layers in Fig. 3(a) have been identified by comparison to the cross-sectional AFM image of Fig. 2 and are indicated by arrows. Figure 3(b) shows the SCM signal cross-sectional profile along the dashed line in Fig. 3(a) and QD layers are also identified by arrows. It is important to bear in mind that in the case of remote doping, electrons in the GaAs spacer layer transfer to the nearest InAs QD layer since the InAs QDs provide the lowest available energy states. As a result, for both direct-doping and remote-doping

This article is copyrighted as indicated in the abstract. Reuse of AIP content is subject to the terms at: http://scitation.aip.org/termsconditions. Downloaded to IP: 137.43.140.249 On: Fri, 22 Nov 2013 16:01:03

cases, the QD layers have higher free electron concentration than the surrounding GaAs barrier layers. Therefore, Figs. 2 and 3 clearly demonstrate that the bright SCM regions correspond to QD layer positions, where high doping is expected, and the dark SCM regions correspond to GaAs barrier positions, where low doping is expected. This result is contrary to the behavior expected from SCM measurements in the dC/dV mode and can be explained by contrast reversal, where the magnitude of the SCM signal is proportional to the free electron concentration in the corresponding region.

There are two primary effects leading to contrast reversal in dC/dV SCM images, namely, surface defects and doping concentration. Both of these effects can combine to flatten the measured C-V curve in low-doped regions only so severely that the measured curve becomes inverted, resulting in contrast reversal.[15–17] While this artifact is undesirable, it is not always possible to choose measuring conditions, especially the dc voltage, to avoid the contrast reversal effect.[15] Surface defects resulting from surface roughness and low-quality surface oxides strongly indicate the occurrence of contrast reversal in SCM measurements.[16] Compared to conventional Si oxides, such surface defects are much more likely to occur in the native GaAs oxide used in this experiment due to the height variation of the sample cross section resulting from the selective etching, and due to the high surface state density of semiconductor-oxide interface trapping charges in the GaAs oxide. The doping concentration below which contrast reversal occurs in low-doped regions is $10^{17}/\text{cm}^3$.[15] This turning point is consistent with the sample heterostructure in which the undoped GaAs barrier layers have extremely low free carrier concentrations ($\sim 10^{14}/\text{cm}^3$)[13] and the InAs QD layers have doping concentrations $\geqslant 5\times 10^{17}/\text{cm}^3$.

Therefore, the SCM image demonstrates contrast reversal and shows the strongest signal for QD layer 4 (12 electrons/dot, remote doping), followed by QD layers 3 (2 electrons/dot, direct doping) and 5 (6 electrons/dot, remote doping). The same features are observed consistently in several scans at different locations. However, the strong SCM signal which appears at the position of QD layer 3 conflicts with the lower doping concentration of 2 electrons/dot. This contradiction suggests electron redistribution may exist in this structure. In order to verify electron redistribution in the sample, the band structure was calculated from the three-dimensional (3D) effective-mass Schrödinger–Poisson method using the NEXTNANO3 semiconductor nanostructure simulation package,[18] as shown in Fig. 3(c). The structural and doping information used in the calculation are based on the parameters of the actual sample. In the calculation, the InAs QD has a dome shape, a height of 6 nm, and a base diameter of 25 nm. The doping position was also specified according to the actual doping position, either direct doping in the QD layer or remote doping in the GaAs barrier for corresponding QD layers. The doping concentration was determined in such a way that the QD in each layer can have 2, 6, or 12 electrons, respectively, according to the actual sample configuration. The simulated band structure shows that a large band bending occurs at the remote-doping position with the highest doping density. A significant band bending (210 meV) originates from QD layer 4, thereby pulling down the conductive band edge of nearby QD layers (layers 3 and 5). As a result, the electrons in this multilayer QD heterostructure are relocated at the QD layers with lower conduction band energy. Therefore, the electrons originally provided by the higher doping concentration in the direct-doping layer (12 electrons in the QD layer 1 and 6 electrons in the QD layer 2) are relocated at QD layer 3, with the lowest conduction band energy. This interpretation is consistent with the SCM image, which shows strongest signal and highest electron concentration in QD layer 3.

Thus, the SCM image and the corresponding band structure calculation lead to a better understanding of doping in QD structures. Namely, electrons provided by direct doping in QDs can be relocated easily due to band structure changes, and such transport may be one of the sources of dark current in QDIPs. Therefore, the cross-sectional SCM technique could be very important in optimizing the doping techniques used during MBE growth of QDIPs in order to enhance device performance.

The authors would like to thank the NEXTNANO3 development team at the Walter Schottky Institute for providing the simulation package and some technical support. A portion of this research was conducted at the Center for Nanophase Materials Sciences, which is sponsored at Oak Ridge National Laboratory by the Division of Scientific User Facilities, U.S. Department of Energy. This work is supported, in part, by the Air Force Office of Scientific Research under Grant No. FA9550-06-1-0482 and the National Science Foundation under Grant No. 0547273.

[1] Z. Y. Zhao, C. Yi, K. R. Lantz, and A. D. Stiff-Roberts, Appl. Phys. Lett. **90**, 233511 (2007).
[2] Z. Y. Zhao, C. Yi, A. D. Stiff-Roberts, A. J. Hoffman, D. Wasserman, and C. Gmachl, J. Vac. Sci. Technol. B **25**, 1071 (2007).
[3] Z. Y. Zhao, C. Yi, A. D. Stiff-Roberts, A. J. Hoffman, D. Wasserman, and C. Gmachl, Infrared Phys. Technol. **51**, 131 (2007).
[4] Z. Y. Zhao, K. R. Lantz, C. Yi, and A. D. Stiff-Roberts, Presented at the Conference on Laser and Electro-Optics, Baltimore, Maryland, 2007 (unpublished).
[5] D. W. Abraham, C. Williams, J. Slinkman, and H. K. Wickramasinghe, J. Vac. Sci. Technol. B **9**, 703 (1991).
[6] C. C. Williams, Annu. Rev. Mater. Sci. **29**, 471 (1999).
[7] S. Anand, IEEE Circuits Devices Mag. **16**, 12 (2000).
[8] K. Maknys, O. Douhéret, and S. Anand, Appl. Phys. Lett. **83**, 4205 (2003).
[9] O. Douhéret, S. Anand, C. Angulo Barrios, and S. Lourdudoss, Appl. Phys. Lett. **81**, 960 (2002).
[10] H. Yamamoto, T. Takahashi, and I. Kamiya, Appl. Phys. Lett. **77**, 1994 (2000).
[11] W. Brezna, T. Roch, G. Strasser, and J. Smoliner, Semicond. Sci. Technol. **20**, 903 (2002).
[12] A. D. Stiff, S. Krishna, P. Bhattacharya, and S. W. Kennerly, IEEE J. Quantum Electron. **37**, 1272 (2001).
[13] C. E. C. Wood, in *The Technology and Physics of Molecular Beam Epitaxy*, edited by E. H. C. Parker (Plenum, New York, 1985), p. 61.
[14] G. Fasching, K. Unterrainer, W. Brezna, J. Smoliner, and G. Strasser, Appl. Phys. Lett. **86**, 063111 (2005).
[15] R. Stephenson, A. Verhulst, P. De Wolf, and M. Caymax, Appl. Phys. Lett. **73**, 2597 (1998).
[16] D. Goghero and V. Raineri, Appl. Phys. Lett. **81**, 1824 (2002).
[17] K. W. Wong, W. K. Chim, and J. Yan, Appl. Phys. Lett. **87**, 053504 (2005).
[18] Nextnano3, Walter Schottky Institute, TU München.

This article is copyrighted as indicated in the abstract. Reuse of AIP content is subject to the terms at: http://scitation.aip.org/termsconditions. Downloaded to IP: 137.43.140.249 On: Fri, 22 Nov 2013 16:01:03